

# Increasing Electron Transfer Rates with Increasing Donor-Acceptor Distance

Martin Kuss-Petermann<sup>[a]</sup> and Oliver S. Wenger<sup>\*[a]</sup>

**Abstract:** Electron transfer can readily occur over long ( $\geq 15$  Å) distances. Usually reaction rates decrease with increasing distance between donors and acceptors, but theory predicts a regime in which electron transfer rates *increase* with increasing reactant separations. This counter-intuitive behavior can result from the interplay of reorganization energy and electronic coupling, but until now experimental studies have failed to provide unambiguous evidence for this effect. We report here on a homologous series of rigid rod-like donor-bridge-acceptor compounds in which the electron transfer rate increases by a factor of 8 when elongating the donor-acceptor distance from 22.0 to 30.6 Å, and then it decreases by a factor of 188 when further increasing the distance to 39.2 Å. This effect has important implications for solar energy conversion.

Electron transfer plays an important role in chemistry, biology, and physics. Many processes indispensable to life, for example photosynthesis and respiration, rely on electron transfer between distant redox partners.<sup>[1]</sup> Collisional encounters between reactants are not needed, because the electron can transfer rapidly over long ( $\geq 15$  Å) distances due to its low mass.<sup>[2]</sup> Usually the rates for electron transfer decrease with increasing distance between reactants.<sup>[3]</sup> More than 30 years ago it was predicted that under certain conditions, electron transfer rates could actually *increase* with increasing distance.<sup>[4]</sup> We report here direct experimental evidence for an electron transfer rate maximum at large reactant separations, compatible with the long-sought effect predicted by theory.

Electron transfer rates ( $k_{ET}$ ) exhibit a Gaussian dependence (Figure 1) on reaction free energy ( $\Delta G_{ET}^0$ ).<sup>[5]</sup> The maximal rate is reached when  $-\Delta G_{ET}^0$  is equal to the reorganization energy ( $\lambda$ ), which is the energy cost associated with solvent and reactant reorganization in the course of electron transfer. When  $-\Delta G_{ET}^0 > \lambda$ , then  $k_{ET}$  decreases with increasing driving-force, and this is known as the “inverted” regime.<sup>[6]</sup>

$$k_{ET} = \sqrt{\frac{\pi}{\hbar^2 \cdot \lambda \cdot k_B \cdot T}} \cdot H_{DA}^2 \cdot \exp\left(-\frac{(\lambda + \Delta G_{ET}^0)^2}{4 \cdot \lambda \cdot k_B \cdot T}\right) \quad (\text{eq. 1})$$

[a] M. Kuss-Petermann, Prof. Dr. O. S. Wenger  
Department of Chemistry  
University of Basel  
St. Johanns-Ring 19, 4056 Basel, Switzerland  
E-mail: oliver.wenger@unibas.ch

Supporting Information for this article is given via a link at the end of the document.

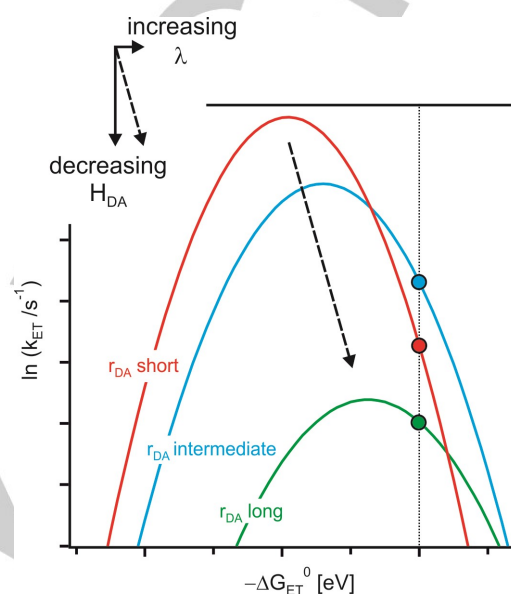


**Figure 1.** Schematic drawing of  $\ln(k_{ET})$  vs.  $-\Delta G_{ET}^0$  showing so-called Marcus parabola. The effect of increasing donor-acceptor distance ( $r_{DA}$ ) on these parabola is illustrated. The maxima of these parabola occur at  $-\Delta G_{ET}^0 = \lambda$ . The dotted vertical line marks a driving-force for which  $k_{ET}$  exhibits a maximum at intermediate distances.

When the distance between donor and acceptor ( $r_{DA}$ ) increases, their electronic coupling ( $H_{DA}$ , middle term in equation 1) usually decreases exponentially, and this leads to an exponential decrease of  $k_{ET}$  with increasing  $r_{DA}$  in the tunneling regime.<sup>[3, 7]</sup> The outer-sphere (solvent) contribution to  $\lambda$  increases with increasing  $r_{DA}$ , because more isolated point charges result when the electron-hole separation distance is larger.<sup>[8]</sup> The combination of a *decrease* of  $H_{DA}$  and an *increase* of  $\lambda$  results in a shift of the driving-force parabola in Figure 1 towards the bottom right corner:<sup>[9]</sup> As  $H_{DA}$  decreases,  $k_{ET}$  must decrease because  $k_{ET} \propto H_{DA}^2$  (eq. 1), shifting the parabolas down. As  $\lambda$  increases, the maximum of the parabola shifts to the right because maximal  $k_{ET}$  is reached when  $-\Delta G_{ET}^0$  is equal to  $\lambda$ . Figure 1 illustrates this effect by showing three generic parabolas, one each for short, intermediate, and long donor-acceptor distances. We note that when  $-\Delta G_{ET}^0$  becomes sufficiently large relative to  $\lambda$ , there can be situations in which  $k_{ET}$  is largest for intermediate  $r_{DA}$  at constant driving-force (dotted vertical line). In other words, as the donor-acceptor distance increases in this regime, the reaction rate should first increase, reach a maximum at a given distance, and then decrease.<sup>[4]</sup>

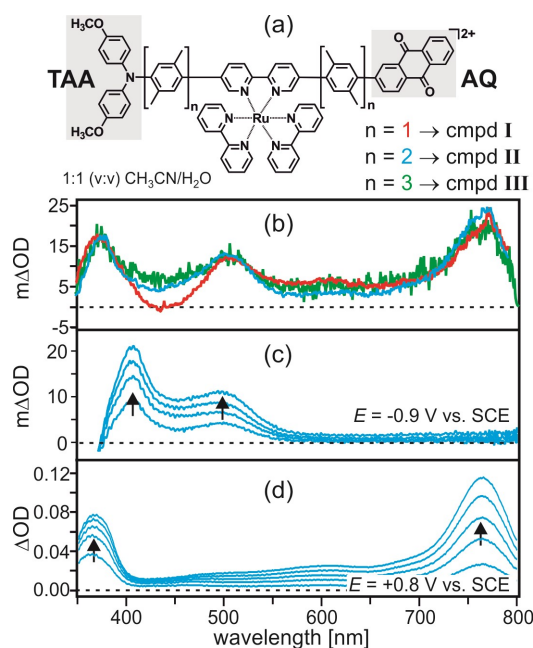


**Figure 2.** (a) Molecular structures of the three key compounds investigated in this work; (b) transient absorption spectra recorded by time-integration over 200 ns following excitation at 532 nm with laser pulses of ~10 ns duration. Red: I, blue: II, green: III (multiplied by a factor of 3.5), sample concentrations were 20  $\mu\text{M}$ . Spectro-electrochemical UV-Vis difference data obtained for II after different time intervals following application of potentials of (c) -0.9 V and (d) +0.8 V vs. SCE leading to formation of (c)  $\text{AQ}^-$  and (d)  $\text{TAA}^+$ , respectively. The UV-Vis spectrum prior to applying any potential served as a baseline, sample concentrations were 0.1 mM. The solvent was deaerated 1:1 (v:v)  $\text{CH}_3\text{CN} / \text{H}_2\text{O}$  at 20  $^\circ\text{C}$  in all cases.

In the three compounds from Figure 2a selective excitation of the  $\text{Ru}(\text{bpy})_3^{2+}$  ( $\text{bpy} = 2,2'$ -bipyridine) photosensitizer induces a rapid sequence of intramolecular electron transfers leading to an oxidized triarylamine ( $\text{TAA}^+$ ) and a reduced anthraquinone ( $\text{AQ}^-$ ). Electron transfer is mediated by  $p$ -xylylene spacers of different lengths ( $n = 1 - 3$ ) which impose a rigid rod-like molecular structure. The transient absorption data in Figure 2b were obtained after excitation at 532 nm with laser pulses of ~10 ns duration. The spectra were recorded by time-integration over 200 ns, either directly after excitation (compounds I, II) or with a time delay of 3  $\mu\text{s}$  (compound III). All three spectra exhibit absorption maxima at 370, 510, and 770 nm, compatible with the formation of  $\text{TAA}^+$  and  $\text{AQ}^-$ , as the comparison with spectro-electrochemical data (Figure 2c/d) shows (SI page S15). All data were recorded in deaerated 1:1 (v:v)  $\text{CH}_3\text{CN} / \text{H}_2\text{O}$  mixture. In compounds I and II, the  $\text{TAA}^+$  and  $\text{AQ}^-$  products form within the duration of the laser excitation pulse, whereas in compound III the time constant for complete formation of the fully charge-separated state is 210 ns (SI pages S16 – S19) hence the use of the 3  $\mu\text{s}$  time delay noted above.

Of key interest in this paper is the kinetics for thermal electron transfer from  $\text{AQ}^-$  to  $\text{TAA}^+$ . This intramolecular charge recombination event has to occur in a single reaction step across 2 – 6  $p$ -xylylene spacers and a bpy ligand. According to molecular modeling, the (center-to-center) donor-acceptor distances are 22.0 (I), 30.6 (II), and 39.2  $\text{\AA}$  (III).

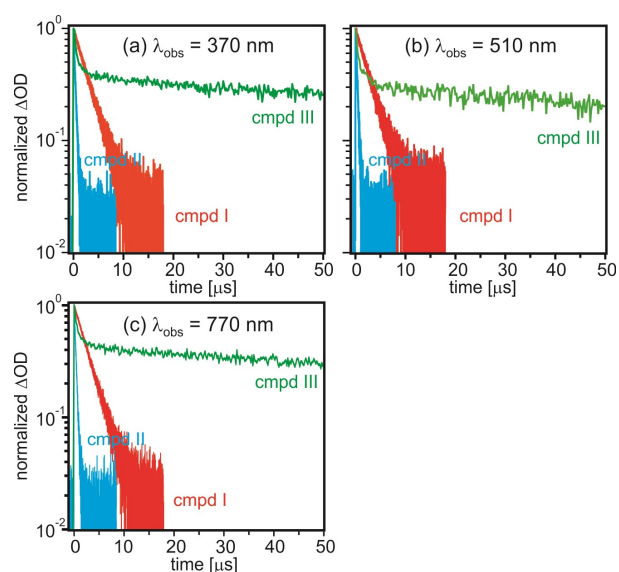


**Figure 3.** Decays of the transient absorption signals at 370 (a), 510 (b), and 770 nm (c) for I (red), II (blue), III (green) in deaerated 1:1 (v:v)  $\text{CH}_3\text{CN} / \text{H}_2\text{O}$  at 20  $^\circ\text{C}$  following excitation at 532 nm with laser pulses of ~10 ns duration. See text and SI pages S16/S17 for explanation of the fast decay component detected for III.

The rates for thermal electron transfer from  $\text{AQ}^-$  to  $\text{TAA}^+$  ( $k_{\text{ET}}$ ) can be extracted from the decays of the transient absorption signals at 370, 510, and 770 nm (Figure 3). For a given compound, at all three wavelengths identical decays are measured, confirming that  $\text{TAA}^+$  (which absorbs at 370 and 770 nm) and hydrogen-bonded  $\text{AQ}^-$  (which absorbs at 370 and 510 nm) disappear simultaneously in one reaction step.  $k_{\text{ET}}$  values extracted from fits to the experimental decay curves are reported in Table 1.

**Table 1.** Center-to-center donor-acceptor distance ( $r_{\text{DA}}$ ), rate constant ( $k_{\text{ET}}$ ), (negative) reaction free energy ( $-\Delta G_{\text{ET}}^0$ ), activation free energy ( $\Delta G_{\text{ET}}^\ddagger$ ), reorganization energy ( $\lambda$ ), and electronic coupling ( $H_{\text{DA}}$ ) associated with thermal electron transfer between  $\text{AQ}^-$  and  $\text{TAA}^+$  in compounds I – III in 1:1 (v:v)  $\text{CH}_3\text{CN} / \text{H}_2\text{O}$ .

cmpd	$r_{\text{DA}}$ [ $\text{\AA}$ ]	$k_{\text{ET}}$ [ $\text{s}^{-1}$ ]	$-\Delta G_{\text{ET}}^0$ [eV]	$\Delta G_{\text{ET}}^\ddagger$ [meV]
I	22.0	$(3.58 \pm 0.36) \cdot 10^5$	$1.33 \pm 0.05$	$43 \pm 2$
II	30.6	$(2.87 \pm 0.29) \cdot 10^6$	$1.29 \pm 0.05$	$-2 \pm 1$
III	39.2	$(1.53 \pm 0.15) \cdot 10^4$	$1.23 \pm 0.05$	$108 \pm 9$
cmpd	$\lambda$ [eV]	$H_{\text{DA}}$ [ $\text{cm}^{-1}$ ]		
I	$0.93 \pm 0.35$	$0.09 \pm 0.02$		
II	$1.29 \pm 0.05$	$0.10 \pm 0.02$		
III	$2.21 \pm 0.28$	$0.08 \pm 0.02$		

For compound II  $k_{\text{ET}}$  is a factor of 8 larger than for compound I, despite the fact that the donor-acceptor distance ( $r_{\text{DA}}$ ) is 8.6  $\text{\AA}$  longer. While compounds I and II yield single-exponential decays, the transient absorption decay of compound III is triple-

exponential at all three detection wavelengths (but only the shorter two out of the three decay components are visible in Figure 3). The shortest of the three time-components is 210 ns and can be attributed unambiguously to the photoinduced charge-separation reaction in which TAA<sup>+</sup> and AQ<sup>-</sup> are formed (SI pages S16/S17; the <sup>3</sup>MLCT excited state of **III** has higher extinction coefficients at the relevant detection wavelengths than the final charge-separated state). The intermediate time-component is 65.4 μs and is attributable to *intramolecular* thermal electron transfer from AQ<sup>-</sup> to TAA<sup>+</sup>, i. e., to the process of main interest. The third time-component (≥ 400 μs; not seen in Figure 3) is caused by *intermolecular* electron transfer reactions (SI pages S20 – S23). Thus, the kinetics for *intramolecular* electron transfer is clear-cut:  $k_{ET}$  increases by a factor of 8 between compounds **I** and **II**, and then decreases by a factor of 188 between **II** and **III**. The reaction free energy ( $\Delta G_{ET}^0$ ) for intramolecular thermal electron transfer from AQ<sup>-</sup> to TAA<sup>+</sup> is very similar in **I**, **II**, and **III** (Table 1, SI page S11).

Temperature-dependence studies of  $k_{ET}$  were performed to determine activation free energies ( $\Delta G_{ET}^\ddagger$ ). From Arrhenius plots the  $\Delta G_{ET}^\ddagger$  values reported in Table 1 were extracted (SI page S24). In compound **II** electron transfer proceeds in essentially activationless manner, whereas in compounds **I** and **III**  $\Delta G_{ET}^\ddagger$  is 43±2 meV and 108±9 meV, respectively. Since  $\Delta G_{ET}^\ddagger = (\lambda + \Delta G_{ET}^0)^2 / 4\lambda$  (equation 1),<sup>[6b]</sup> reorganization energies ( $\lambda$ ) can be determined from these values. In the case of **II**,  $\lambda$  must be equal to  $-\Delta G_{ET}^0$  (1.29±0.05 eV) because the reaction is barrierless. For compounds **I** and **III**, the quadratic relationship between  $\Delta G_{ET}^\ddagger$  and  $\lambda$  yields two mathematical solutions, but in each case only one solution is physically meaningful because  $\lambda$  is expected to increase with increasing  $r_{DA}$  (SI pages S26, S34).<sup>[4a, 8, 10]</sup> Thus we obtain  $\lambda = 0.93\pm 0.35$  eV for **I**, 1.29±0.05 eV for **II**, and 2.21±0.28 eV for **III** in 1:1 (v:v) CH<sub>3</sub>CN / H<sub>2</sub>O (Table 1).

The dominant contribution to  $\lambda$  usually comes from the outer-sphere reorganization energy ( $\lambda_o$ ), while the inner-sphere contribution is small and largely independent on  $r_{DA}$ .<sup>[10]</sup> Simple two-sphere electrostatic models fail to quantitatively reproduce the experimentally observed increase in  $\lambda$  for compounds **I** – **III** in 1:1 (v:v) CH<sub>3</sub>CN / H<sub>2</sub>O,<sup>[8, 11]</sup> because they do not take hydrogen-bonding into account. Direct evidence for the importance of hydrogen-bonding in our systems comes from the AQ<sup>-</sup> related transient absorption band at 510 nm (Figure 2b/c). In neat CH<sub>3</sub>CN, this band appears at 565 nm for compounds **I** – **III**, (SI page S27) and the shift to shorter wavelength in 1:1 (v:v) CH<sub>3</sub>CN / H<sub>2</sub>O is in line with hydrogen-bond donation from water.<sup>[12]</sup> Based on prior electrochemical studies and on calculations for benzoquinone radical anion, we expect that 4 – 5 H<sub>2</sub>O molecules are involved in hydrogen-bonding to AQ<sup>-</sup>,<sup>[13]</sup> and this raises  $\lambda$  significantly with respect to what is predicted by a simple dielectric continuum model.<sup>[8, 11]</sup> The further AQ<sup>-</sup> is spatially separated from cationic charges (Ru(bpy)<sub>3</sub><sup>2+</sup>, TAA<sup>+</sup>), the more important the effect of hydrogen-bonding becomes. For comparison, a study of phototriggered phenol oxidation found  $\lambda = 2.0$  eV because the phenolic O-H bond was broken in the course of electron transfer.<sup>[14]</sup>

In neat CH<sub>3</sub>CN the reorganization energy ( $\lambda$ ) for compound **III** is only 1.62±0.05 eV because no hydrogen-bonding to AQ<sup>-</sup> can occur (SI page S33). We note that the change from 1:1 (v:v)

CH<sub>3</sub>CN / H<sub>2</sub>O to neat CH<sub>3</sub>CN does also alter the driving-force for thermal charge-recombination in a significant manner (~0.3 eV) because non-hydrogen bonded AQ<sup>-</sup> is easier to oxidize than its hydrogen-bonded analogue, and TAA<sup>+</sup> reduction is more facile in neat CH<sub>3</sub>CN (SI page S13). Thus, solvent changes do not only affect  $\lambda$ , but they also lead to significant changes of  $\Delta G_{ET}^0$  in our compounds (SI page S36). As  $\Delta G_{ET}^0$  for charge-recombination increases, the driving-force for photoinduced charge-separation decreases, because the energy of the initially populated <sup>3</sup>MLCT excited state remains relatively constant. In CH<sub>2</sub>Cl<sub>2</sub> and more apolar solvents one reaches a point at which efficient charge-separation is no longer possible in compounds **II** and **III**. This precludes further solvent dependence studies.

With the  $\lambda$ ,  $\Delta G_{ET}^0$ , and  $k_{ET}$  values from Table 1 for 1:1 (v:v) CH<sub>3</sub>CN / H<sub>2</sub>O mixtures at hand, equation 1 can be used to obtain estimates of  $H_{DA}$ . We find that the electronic coupling is only very weakly distance dependent with  $H_{DA}$  values of 0.09±0.02 cm<sup>-1</sup> (**I**), 0.10±0.02 cm<sup>-1</sup> (**II**), and 0.08±0.02 cm<sup>-1</sup> (**III**). At first glance this is a somewhat unexpected result, particularly in view of prior studies of donor-acceptor compounds with oligo-*p*-xylene bridges which have produced distance decay constants ( $\beta$ ) between 0.52 – 0.77 Å<sup>-1</sup> for  $k_{ET}$ .<sup>[15]</sup> However, the earlier studies have exclusively focused on photoinduced (forward) electron transfer in the so-called normal regime. It has been noted earlier that the kinetics of photoinduced (forward) electron transfer and thermal (reverse) electron transfer can exhibit significantly different distance dependences, because the superexchange coupling pathways (determining the magnitude of  $H_{DA}$ ) can be fundamentally different.<sup>[9, 16]</sup> We suspect that the weak distance dependence of  $H_{DA}$  in compounds **I** – **III** is due to increasing  $\pi$ -conjugation between the central bpy and adjacent *p*-xylene units with increasing length. This interpretation is supported by the observation that the spectroscopic signature of the <sup>3</sup>MLCT state of a reference complex lacking the AQ and TAA components but bearing *p*-xylene bridging units is substantially different from the <sup>3</sup>MLCT spectrum of Ru(bpy)<sub>3</sub><sup>2+</sup> (SI page S19).

Because of the initial population of a <sup>3</sup>MLCT excited state, a radical ion pair (AQ<sup>-</sup> / TAA<sup>+</sup>) with triplet spin multiplicity forms initially. Charge-recombination must occur directly to the singlet ground state, but spin effects are not expected to play a decisive role as far as the distance dependence of  $k_{ET}$  is concerned. Possible spin and electron-vibration coupling effects are discussed in the SI (pages S38 – S41).<sup>[6b, 16b, 17]</sup>

In conclusion, the highly unusual observation of an electron transfer rate maximum at large (30.6 Å) reactant separation can be explained by a weak distance dependence of electronic donor-acceptor coupling ( $H_{DA}$ ) combined with a strong distance dependence of the reorganization energy ( $\lambda$ ), as predicted by theory more than 3 decades ago.<sup>[4a]</sup> As  $\lambda$  increases with increasing donor-acceptor distance, our reaction systems pass through the inverted (**I**), barrierless (**II**), and normal (**III**) regimes of electron transfer, and all the while the reaction free energy ( $\Delta G_{ET}^0$ ) stays essentially constant (Figure 4), in marked contrast to prior driving-force dependence studies.<sup>[6]</sup>

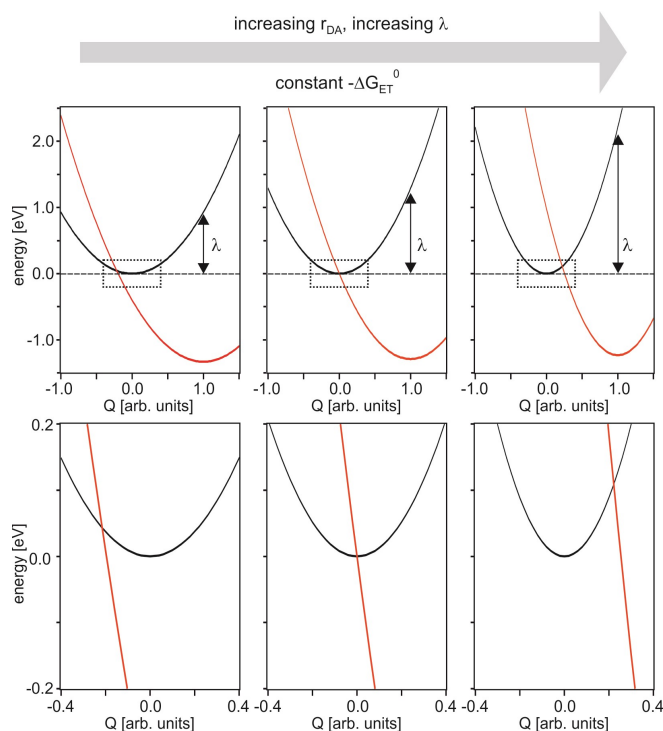


**Figure 4.** Reactant (black) and product (red) potential energy wells illustrating the changeover from inverted (left) to activationless (middle) to normal (right) electron transfer as a function of increasing distance ( $r_{DA}$ ) between AQ $\cdot$  and TAA $\cdot$  in compounds I, II, and III. The driving-force ( $-\Delta G_{ET}^0$ ) stays nearly constant (Table 1), the changeover is essentially due to increasing reorganization energy ( $\lambda$ ) with increasing  $r_{DA}$ . The lower half of the figure shows zooms of the regions marked by dotted rectangles in the upper half.

The simple model illustrated in Figure 4 is fully compatible with the experimentally observed rate constants, reaction free energies, and activation free energies. We are unaware of prior studies that have observed a rate maximum at large distances, caused by a changeover from inverted to barrierless to normal electron transfer as a function of  $r_{DA}$ .

The effect observed herein is not merely an oddity of purely academic interest, but it has important practical implications. Photoinduced electron transfer between a donor (D) and an acceptor (A) leads to electron-hole pairs (D $^+$ , A $^-$ ), a form of chemically stored energy.<sup>[18]</sup> These light-induced reactions commonly occur in the normal regime where  $-\Delta G_{ET}^0 < \lambda$ , hence in bimolecular processes they take place preferentially when reactants are in close contact ( $r_{DA} \leq 10$  Å), because in the normal regime  $k_{ET}$  simply decreases with increasing  $r_{DA}$ .<sup>[4]</sup> When aiming to convert solar light into chemical energy, it is then desirable that oxidation (D $^+$ ) and reduction products (A $^-$ ) diffuse away from each other without undergoing direct charge-recombination. However, such energy-wasting processes often occur in the inverted driving-force regime at close contact. Consequently, as the distance between the D $^+$  and A $^-$  photoproducts increases in the course of diffusion, the rate for charge-recombination is increasing until a critical separation distance is reached (i. e., the  $r_{DA}$  for which  $-\Delta G_{ET}^0 = \lambda$ ). Only past that point does the charge-recombination rate decrease

with increasing  $r_{DA}$ . This can severely limit the quantum efficiency of light-to-chemical energy conversion.

## Acknowledgements

This research was funded by the Swiss National Science Foundation (grant number 200021\_146231/1).

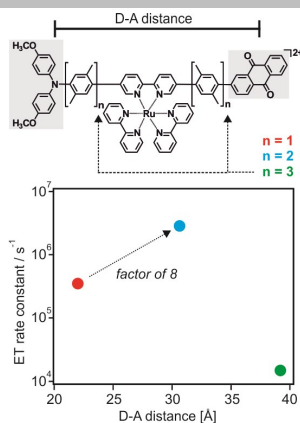
**Keywords:** electron transfer • donor-acceptor systems • time-resolved spectroscopy • photochemistry • energy conversion

- [1] a) D. De Vault, B. Chance, *Biophys. J.* **1966**, *6*, 825-847; b) J. R. Winkler, H. B. Gray, *Chem. Rev.* **1992**, *92*, 369-379; c) M. R. Wasielewski, *Chem. Rev.* **1992**, *92*, 435-461; d) C. C. Moser, J. M. Keske, K. Warncke, R. S. Farid, P. L. Dutton, *Nature* **1992**, *355*, 796-802.
- [2] H. B. Gray, J. R. Winkler, *Proc. Natl. Acad. Sci. U. S. A.* **2005**, *102*, 3534-3539.
- [3] a) P. P. Edwards, H. B. Gray, M. T. J. Lodge, R. J. P. Williams, *Angew. Chem. Int. Ed.* **2008**, *47*, 6758-6765; b) M. Cordes, B. Giese, *Chem. Soc. Rev.* **2009**, *38*, 892-901.
- [4] a) B. S. Brunschwig, S. Ehrenson, N. Sutin, *J. Am. Chem. Soc.* **1984**, *106*, 6858-6859; b) M. Tachiya, S. Murata, *J. Phys. Chem.* **1992**, *96*, 8441-8444; c) S. Murata, M. Tachiya, *J. Phys. Chem.* **1996**, *100*, 4064-4070.
- [5] R. A. Marcus, N. Sutin, *Biochim. Biophys. Acta* **1985**, *811*, 265-322.
- [6] a) M. R. Wasielewski, M. P. Niemczyk, W. A. Svec, E. B. Pewitt, *J. Am. Chem. Soc.* **1985**, *107*, 1080-1082; b) G. L. Closs, J. R. Miller, *Science* **1988**, *240*, 440-447; c) L. S. Fox, M. Kozik, J. R. Winkler, H. B. Gray, *Science* **1990**, *247*, 1069-1071.
- [7] a) J. R. Miller, J. A. Peebles, M. J. Schmitt, G. L. Closs, *J. Am. Chem. Soc.* **1982**, *104*, 6488-6493; b) M. D. Newton, *Chem. Rev.* **1991**, *91*, 767-792.
- [8] R. A. Marcus, *J. Chem. Phys.* **1965**, *43*, 679-701.
- [9] E. H. Yonemoto, G. B. Saupe, R. H. Schmehl, S. M. Hubig, R. L. Riley, B. L. Iverson, T. E. Mallouk, *J. Am. Chem. Soc.* **1994**, *116*, 4786-4795.
- [10] S. S. Isied, A. Vassilian, J. F. Wishart, C. Creutz, H. A. Schwarz, N. Sutin, *J. Am. Chem. Soc.* **1988**, *110*, 635-637.
- [11] J. G. Kirkwood, F. H. Westheimer, *J. Chem. Phys.* **1938**, *6*, 506-512.
- [12] a) B. E. Hulme, G. O. Phillips, E. J. Land, *J. Chem. Soc., Faraday Trans.* **1972**, *68*, 1992-2002; b) J. Hankache, M. Niemi, H. Lemmetyinen, O. S. Wenger, *J. Phys. Chem. A* **2012**, *116*, 8159-8168.
- [13] a) M. Quan, D. Sanchez, M. F. Wasylkiw, D. K. Smith, *J. Am. Chem. Soc.* **2007**, *129*, 12847-12856; b) S. Sinnecker, E. Reijerse, F. Neese, W. Lubitz, *J. Am. Chem. Soc.* **2004**, *126*, 3280-3290; c) N. Gupta, H. Linschitz, *J. Am. Chem. Soc.* **1997**, *119*, 6384-6391.
- [14] M. Sjödin, S. Styring, B. Åkermark, L. C. Sun, L. Hammarström, *J. Am. Chem. Soc.* **2000**, *122*, 3932-3936.
- [15] a) D. Hanss, O. S. Wenger, *Inorg. Chem.* **2008**, *47*, 9081-9084; b) D. Hanss, O. S. Wenger, *Inorg. Chem.* **2009**, *48*, 671-680; c) O. S. Wenger, B. S. Leigh, R. M. Villahermosa, H. B. Gray, J. R. Winkler, *Science* **2005**, *307*, 99-102.
- [16] a) B. Albinsson, M. P. Eng, K. Pettersson, M. U. Winters, *Phys. Chem. Chem. Phys.* **2007**, *9*, 5847-5864; b) J. Sukegawa, C. Schubert, X. Z. Zhu, H. Tsuji, D. M. Guldi, E. Nakamura, *Nature Chem.* **2014**, *6*, 899-905; c) A. Arrigo, A. Santoro, F. Puntoriero, P. Lainé, S. Campagna, *Coord. Chem. Rev.* **2015**, *304-305*, 109-116; d) M. Natali, S. Campagna, F. Scandola, *Chem. Soc. Rev.* **2014**, *43*, 4005.
- [17] M. Delor, T. Keane, P. A. Scattergood, I. V. Sazanovich, G. M. Greetham, M. Towrie, A. Meijer, J. A. Weinstein, *Nature Chem.* **2015**, *7*, 689-695.
- [18] I. R. Gould, D. Ege, J. E. Moser, S. Farid, *J. Am. Chem. Soc.* **1990**, *112*, 4290-4301.

## Entry for the Table of Contents

## COMMUNICATION

Usually electron transfer rates decrease with increasing donor-acceptor separation. However, the interplay between reorganization energy and electronic coupling can lead to opposite, counter-intuitive behaviour.



Martin Kuss-Petermann, Oliver S. Wenger\*

Page No. – Page No.

**Increasing Electron Transfer Rates  
with Increasing Donor-Acceptor  
Distance**